

STRUCTURAL CHARACTERISATION AND OPTICAL PROPERTIES OF CdCl₂ DOPPED POLYANILINE

SUBRAMANYA KILARKAJE ¹, PAVITHRA G M ²

¹Department of Physics, Sahyadri Science College, Kuvempu University, Shankaraghatta-577 451, Shimoga, Karnataka, INDIA.

²Department of Mathematics, Sahyadri Science College, Kuvempu University, Shankaraghatta-577 451, Shimoga, Karnataka, INDIA.

Abstract

According to this work, CdCl₂ doped polyaniline was synthesised using chemical synthesis at varied dopant weight percentages. The optical absorption of pure and CdCl₂ doped Polyaniline was investigated using a UV-visible spectrometer over the wavelength range 190–800nm. The chemical interactions, structure, and morphology of pure and doped PANI were investigated using SEM, X-ray diffraction, and Fourier Transform Infrared (FTIR) spectroscopy (SEM). Due to the dopant, the UV-vis absorption data were recorded by the Shimadzu 2550 (UV 1800 ENG 240V) UV-Visible Spectrophotometer. UV-Visible absorption spectra were utilised to determine the optical energy, direct and indirect band gaps, and other spectral properties. The optical band gap energy decreases to 2.35 eV as the dopant concentration increases. The size of the carbonaceous cluster is defined by a modified version of Tauc's equation, and it expands proportionally to the dopant concentration. The doped PANI results show a change in the FTIR peaks at 2923cm⁻¹ and 1226cm⁻¹. When the concentration of dopants is increased, the 2θ value shifts and the intensity of doped films increases. As evidenced by the SEM results, the PANI's surface morphology altered consistently with dopant.

Keywords: Polyaniline, Optical properties, chemical interaction, morphology, Band Gap

1.INTRODUCTION

Researchers have recently focused their attention on conjugated polymers because to their superior electrical conductivity and optical characteristics as a result of doping. It is unusual among conducting polymers due to its environmental stability, simplicity of obtaining raw materials, affordable synthesis technique, and -conjugated electrons scattered throughout the polymer backbone. To enhance the polymer's electrical, optical, and mechanical capabilities, electrons are distributed more extensively along the polymer chain.

There are very few polyaniline conductors in existence, and polyaniline is one of the most stable and widely used. In addition to its wide range of potential applications in organic light emitting diodes [1-4], molecular sensors, nonlinear optical devices, electrochromic displays and microelectronic devices, it is a significant conducting polymer due to its ease of processing, environmental stability, low cost and oxidation- or protonation-adjustable electrical properties.

Polyaniline can be synthesised chemically or electrochemically via oxidative polymerization of aniline monomer [16]. Chemical polymerization can yield large volumes of polyaniline, but electrochemical synthesis can only yield a polyaniline layer on the anode; in this case, we used the chemical method. In this work, various doses of cadmium chloride doped polyaniline were synthesised. This article discusses the optical properties of doped polyaniline and the effect of the dopant on chemical interaction, structural, morphological, and structural features.

Researchers have been experimenting with various chemical ways to improve the optical and electrical properties of polyaniline for several years, including doping it with various inorganic alkali and metal salts, such as FeCl_3 , NiCl_2 , LaCl_3 , anilinium chloride, and $\text{ZrO}_2/\text{PbI}_2$ [17, 18]. Epstein et al. [20], Roa et al. [21], and McCall et al. [22] all performed absorption measurements on polyaniline emerald base. Chemically synthesised PANI/Cd dopants in a range of concentrations were used in the current work. The optical, chemical, structural, and morphological properties of the PANI/Cd dopant were all discussed.

2. EXPERIMENTAL

2.1. Synthesis of Polyaniline

It is necessary to chill the aniline solution to between 0 and 3 degrees Celsius before adding the ammonium peroxy sulphate disulphate (0.1 mole in protonic acid) drop by drop to the hydrochloric acid solution (1.0 mole). In order to acidify the aniline slurries, the aqueous solution of hydrochloric acid is dissolved in 1 mole of cadmium chloride salt and the dissolved solution is added. Slowly adding ammonium peroxy sulphate solution prevents the solution from warming up. A mechanical stirrer is used to keep the reaction going for 24 hours after the addition is complete. Protonic acid and temperature are two factors that affect the time it takes for the reaction to begin colouring. Hydrochloric acid is employed as a protonic acid in this polymerization procedure, and a freezing mixture is used to keep the temperature between 0 and 2 degrees Celsius. In order to eliminate the unreacted aniline from the solution and obtain the Emeraldine salt form of PANI, the filtrate was washed with 1M HCl and dried at 60°C in vacuum before being converted into the base form by dedoping with 0.1M NH_4OH solution. The PANI produced by this approach is dark green in colour and has a protonated state. The precipitate was allowed to equilibrate with an adequate amount before being dried, weighed, and then weighed.

The sequence of colorisation is

light blue → blue green → coppery tinny → green precipitates

2.2. CHARACTERISATION

The XRD patterns of PANI were recorded using an X-ray Powder Diffractometer (Bruker AXS D8 Advance Cu, wavelength 1.5406 \AA) at a scanning rate of 10 per minute. The chemical structure of a pure and doped polymer was determined using Fourier transform infrared (FTIR) spectra recorded on a Perkin Elmer FT-IR Spectroscopy in the range $450\text{--}4000 \text{ cm}^{-1}$. The optical absorption spectra of pure PANI and doped PANI were determined at room temperature using a Shimadzu 2550 (UV 1800 ENG 240V) UV-Visible Spectrophotometer. By dissolving a trace amount of pure and doped polyaniline in N-methyl pyrrolidone (NMP) solvent, UV-vis spectroscopy-ready samples were obtained.

3. DISCUSSIONS OF RESULTS

3.1. Analysis of XRD

Figure 1 depicts the X-ray diffraction patterns of pure and doped PANI. The summits are clearly visible positioned at $2\theta=9.54^\circ$, 18.54° and 25.70° for pure PANI.

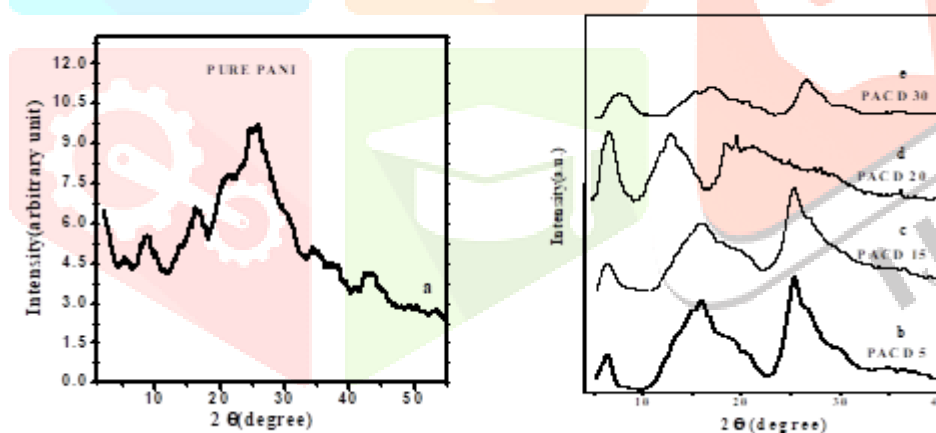


Figure 1. X-ray diffraction pattern of a) pure PANI, and b) PACD 5, c) PACD 15, d) PACD 20, e) PACD 30, wt % of CdCl₂.

1. The broad diffraction peaks observed that the 2θ value found to be decreases i.e., $2\theta=15.95^\circ, 15.92^\circ, 12.79^\circ, 15.21^\circ$ and $2\theta=25.43^\circ, 25.20^\circ, 19.11^\circ, 25.62^\circ$ for PACD 5, PACD 15, PACD 20, and PACD 30 respectively. As CdCl₂ salt levels in the polymer increase, the peaks get darker. Polymer electrolyte crystallinity decreases as the crystallite size decreases, and the amorphous nature of the polymer electrolyte rises with the addition of dopant concentration [23-24].
2. A connection was found between peak intensity and crystallinity by Hodge et al. [25]. A drop in XRD pattern intensity was found as the amorphous form of salt was increased.
3. As CdCl₂ salt levels in the polymer increase, the peaks get darker. In other words, as the crystallite size of the polymer electrolyte is reduced, the crystalline phase decreases [26].
4. Higher quantities of CdCl₂ salt in the polymer did not show any strong peaks, indicating the predominance of amorphous phase [27].

3.2 FTIR-SPECTROSCOPY:

FTIR is a valuable tool in polymer research for analysing local structural changes and interactions. This method can be used to analyse the composition, production, and behaviour of polymeric materials. The complexation and interaction of various constituents can be observed in the materials' infrared spectra, which changes according to their composition. The technique known as infrared spectroscopy was used to determine the intermolecular and intramolecular interactions between the components of the polymer–salt complexes. When atoms or molecules in a material undergo vibrational mode changes, its physical and chemical characteristics may be altered as a result. A representation of pure polyaniline's infrared spectrum is displayed in the figure. The principal distinctive peaks of Quinoid - Benzenoid N moieties for the C-N stretching and C-H aromatic in-plane and out-of-plane bending vibrations of polyaniline are reported to be at around 1656cm^{-1} , 1569 , 1309 , 1109 , and 795cm^{-1} [28].

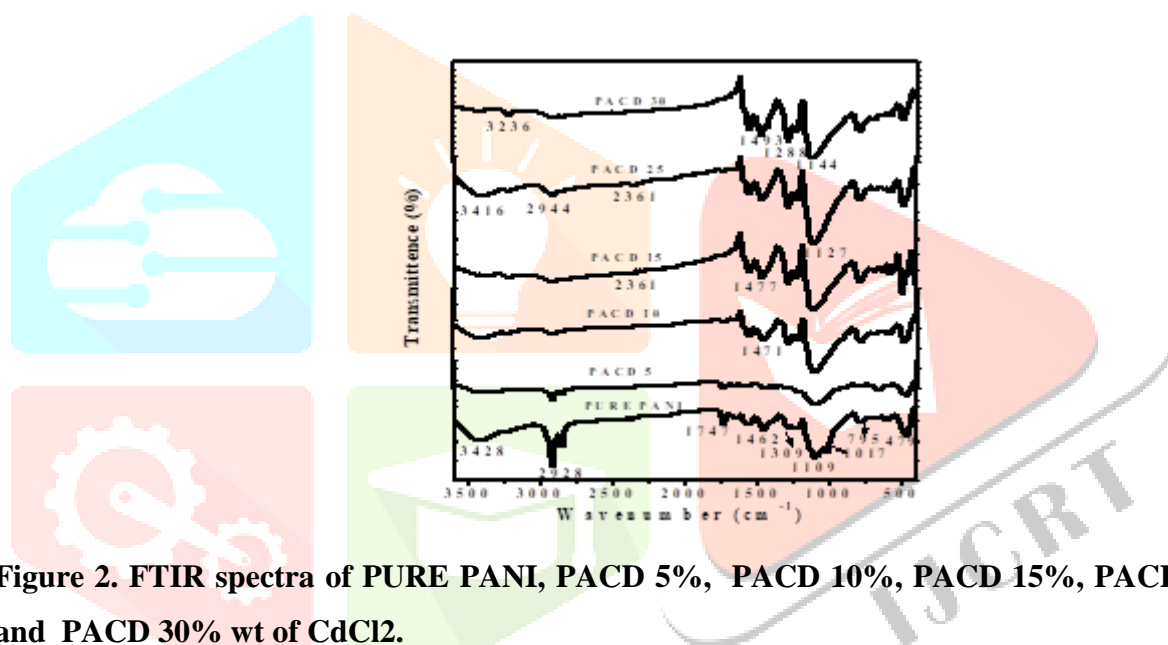


Figure 2. FTIR spectra of PURE PANI, PACD 5%, PACD 10%, PACD 15%, PACD 25%, and PACD 30% wt of CdCl₂.

The figure 2. illustrates the PANI characteristic peaks for C-N stretching, C-H aromatic in-plane and out-of-plane bending vibrations of Quinoid –Benzenoid N moieties at 1656cm^{-1} , 1569 , 1309 , 1109 , and 795cm^{-1} , respectively. Doped PANI peaks at 1570cm^{-1} (the aromatic C=C stretching of the quinonoid (Q-ring), 1465cm^{-1} (the aromatic C=C stretching of the benzenoid (B) ring), 1309cm^{-1} (the C–N stretching of the secondary aromatic amine), 1235cm^{-1} (C–N⁺ stretching), 1140cm^{-1} (B–NH⁺=Q stretching), and 805cm^{-1} (the aromatic C– The broad band observed between 3500 and 2800cm^{-1} is mostly due to N–H stretching vibrations of the secondary amine in the PANI backbone, as well as hydrogen-bonded N–H stretching. Finally, it is noted that the FTIR data indicate a shift in the peaks at 2928cm^{-1} and 1109cm^{-1} , indicating the presence of dopant[29].

3.3 MORPHOLOGY:

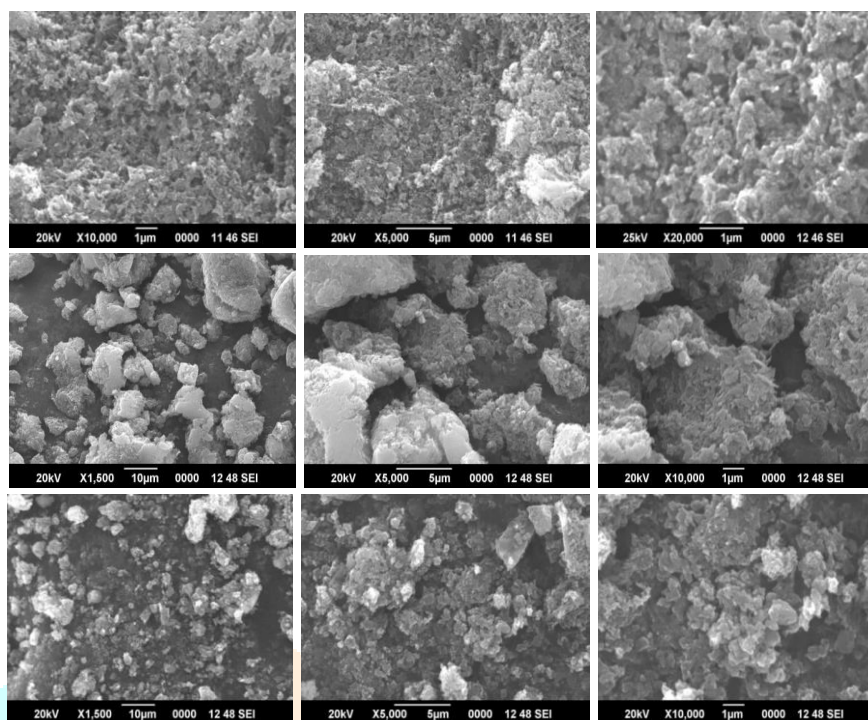


Figure 3. SEM image of the PANI, PACD 5, & 30% wt of CdCl₂.

The morphology of Doped Pani is highly erratic, with both large and small grains. There may have been a surplus of dopant that did not react with Pani, resulting in the big particles. There is a sponge-like structure to the particles, and each layer of morphology has varied dimensions. The porosity nature of the surface is diminished, and the surface shows fine, uneven grains. The substance has lumps and holes evident in its surface, indicating that the surface is not smooth. Gas adsorption is enhanced by the uneven surface's texture.

3.4. OPTICAL-SPECTROSCOPY:

3.4.1. ABSORBANCE

The absorption spectra of doped PANI in the wavelength range 190-900nm are presented in Figure 4. The PANI salt is insoluble in the majority of organic solvents, with the exception of DMSO, DMF, THF, and NMP, which may have some solubility. The electronic absorption spectrum of PANI was determined in this study by dissolving it in NMP solution. Two broad electronic absorption bands, one at 350–412nm and one around 620–650nm, are identified, with similar results to those reported previously [30]. The first band $\pi \rightarrow \pi^*$ corresponds to the amine's transition state, whereas the latter corresponds to the excitation of the PANI backbone's imine units.

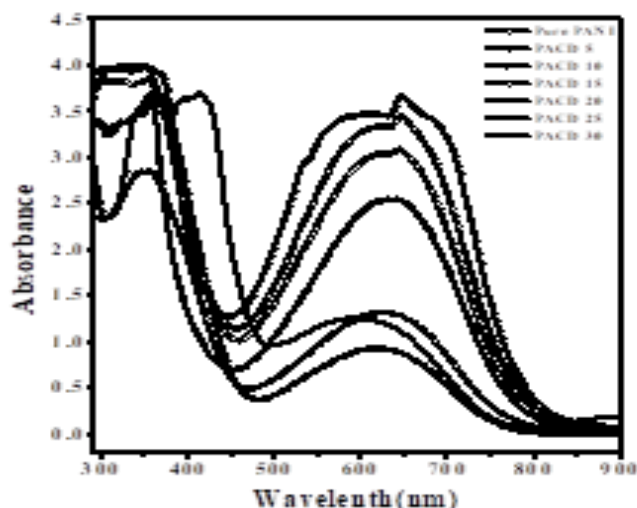


Figure 4. Plot of Absorbance versus wavelength of Pure PANI, PACD 5, PACD 10, PACD 15, PACD 20, PACD 25 and PACD30 weight percentages of CdCl₂.

3.4.2 OPTICAL ABSORPTION COEFFICIENT

With the help of the formula (1), we were able to calculate the optical absorption coefficient. The absorbance was used to compute the absorption coefficient. The absorption coefficient was calculated using the relation after reflection had been corrected.

$$\alpha(\nu) = 2.303 \frac{A}{d} \quad (1)$$

Here, A is the amount of light that can be absorbed by the film.

3.4.3 OPTICAL BAND GAP

When you look at how light is absorbed by a material, you can figure out its band structure. Direct band gap and indirect band gap are the two main types of insulators/semiconductors, and they are the two main types. When a direct band gap semiconductor is made, it has zero crystal momentum in both of its bands (wave vector). An "indirect band gap semiconductor" is one where the bottom of the conduction band does not correspond to zero crystal momentum. This is called a semiconductor with a "indirect band gap." Indirect band gap materials must always have the right amount of crystal momentum when they move from the valence band to the conduction band, or else they won't work. Davis and Shalliday said that, near the fundamental band edge, both direct and indirect transitions happen. This can be seen by plotting $\alpha^{1/2}$ & α^2 as a function of energy and looking at how they change (hv). It is based on the following relationships in Thutupalli and Tomlin [31].

In order to determine the band structure of a substance, one must first examine how that material absorbs light. There are two primary categories of insulators/semiconductors: direct band gap and indirect band gap. Direct band gap and indirect band gap are indeed the two primary types. When a semiconductor with a direct band gap is manufactured, it has zero crystalline momentum in both its bands (wave vector). It is referred to as a "band gaps semiconductor" if the base of the bandgap does not correlate to zero crystal momentum at the same time. This type of semiconductor is referred described as having a "indirect band gap." In order for band gaps materials to function properly, they must have always had the appropriate amount of crystalline momentum as they transition from the valance band band. In their research, Davis and Shalliday discovered that transitions between direct and indirect modes occur at the fundamental band's boundary. By charting $\alpha^{1/2}$ & α^2 as functions of energy, and seeing how they vary, we can see what is going on (hv). Thutpalli and Tomlin [31] established the following relationships as the foundation for their theory.

$$(\alpha hv)^2 = C(hv - E_{gd}) \quad (2)$$

$$(\alpha hv)^{1/2} = C(hv - E_{gi}) \quad (3)$$

In this example, the letters C stand for photon energy, direct band gaps, band gaps, absorption coefficient, as well as a collection of constants. The photon energy is referred to as hv. It is possible to use these terminologies to describe either direct and indirect transitions in a material, which can aid in the determination of the band structure of the material.

When there is a direct gap, the absorption coefficient does have the following relationship to the energy of the photons that enter it, according to the Mott and Davis Model [33]: Whenever there is a direct gap, the absorption coefficient has the following relation to a energy of the photons that enter it:

$$\alpha hv = C(hv - E_g)^{1/2} \quad (4)$$

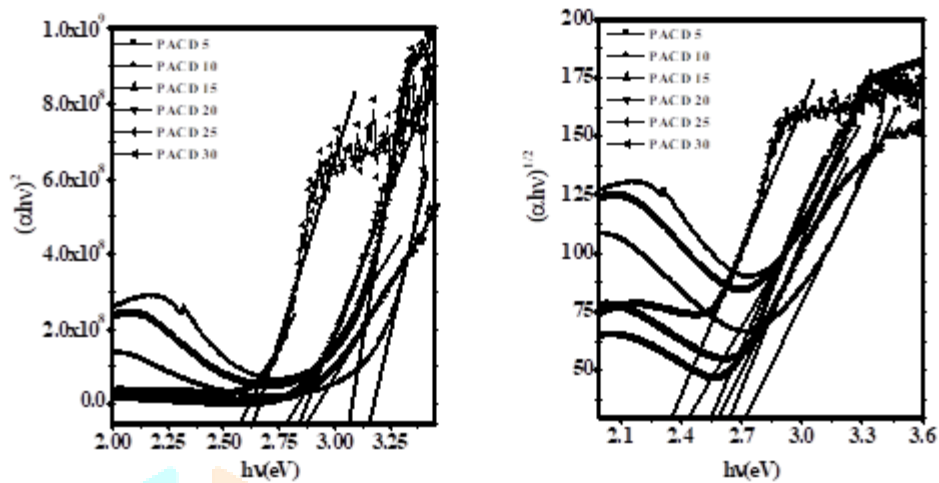
Where E_g denotes the band gap, C ($C = 4\pi\sigma_o/nc\Delta E$) is a constant that depends on the spectrum structure, ν is the incident light frequency, and h denotes the Plank's constant. Thus, a plot of $(\alpha hv)^2$ vs. photon energy (hv) should be linear, as illustrated in figure 5. The bandgap value can be calculated from the intercept just on energy obtained by extending the linear portion of the curves until zero absorption. As indicated in Table 1, the straight band gap of pure film is 4.15eV, but the values for doping polymer would be between 3.38 and 2.24eV, respectively.

According to the following relationship, the absorption coefficient for indirect transitions that necessitate photon aid is proportional to photon energy.

$$\alpha hv = A[hv - E_g + E_p] + B[hv - E_g + E_p]^2 \quad (5)$$

A and B are constants based on the band structure, and E_p is the energy of the photon associated with the transition. Figure 5 shows the plots of $(\alpha hv)^{1/2}$ vs photon energy that yielded the indirect band gaps, which were then tallied in Table (1).

Table: 1. For various weight percent of CdCl₂ doped PANI, direct and indirect band gaps, as well as the amount of carbon atoms in a cluster, were measured.



Sample	Direct band gap (E _g)	Number of Carbon atoms in clusters (N)	Indirect band gap (E _g)	Number of Carbon atoms in clusters (N)
PACD 5	3.16	5.76	2.73	6.67
PACD 10	3.06	5.95	2.65	6.87
PACD 15	2.88	6.32	2.59	7.03
PACD 20	2.84	6.41	2.54	7.17
PACD 25	2.79	6.53	2.44	7.46
PACD 30	2.57	7.09	2.34	7.78

Figure 5. Plot of $(\alpha h\nu)^2$ and $(\alpha h\nu)^{1/2}$ versus photon energy of CdCl₂ doped Polyaniline.

3.4.4 CARBONACEOUS CLUSTERS:

The following equation gives the number of carbon atoms per length of conjugation N for a linear structure, where N is proportional to the optical energy band gap E_g:

$$N = \frac{2\beta\pi}{E_g} \quad (6)$$

Where 2β is the energy of a pair of adjacent π sites and β is taken to be -2.9 eV as it is associated with the π → π* optical transition in the -C=C-structure [34]

As indicated in Table 1, the number of carbon atoms per conjugation length (N) changes when PANI is doped with CdCl₂ or not. Increases in dopant are shown to increase the number of carbon atoms in the clusters. The release of hydrogen is caused by the breakdown of C-H bonds during doping. If there is an impurity or defect state within the gap that causes the band tail in amorphous materials, it is well recognised that these materials have a range of faults and dislocations.

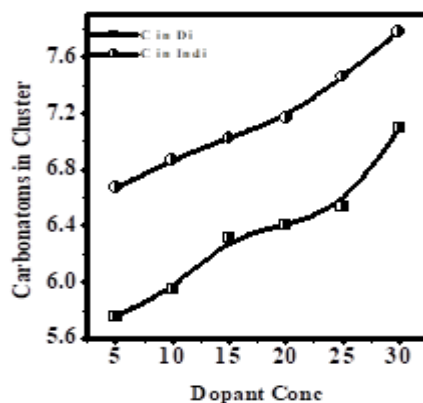


Figure 5. The variation of Carbon atoms in cluster versus weight percentages of CdCl₂ dopant.

UV spectral analysis on these samples shows that the CdCl₂ doped PANI is suitable for potential device applications [36].

CONCLUSIONS

Doping PANI with CdCl₂ changed its optical characteristics, and the results are summarised as follows:

The amorphous nature of the CdCl₂ doped PANI is to blame for the drop in peak intensity, which is caused by an increase in the CdCl₂ concentration. CdCl₂'s weight percentage had a considerable effect on the relative strength of various diffraction pattern peaks. Cluster groups are to blame for the reduction in both direct and indirect energy gaps. Metal ion doping into the polymer is suitable for prospective device applications, as shown by UV spectrum analysis on these samples. The existence of functional groups has been confirmed by FTIR spectral analysis, and the IR spectra show that PANI has been complexed with CdCl₂. For direct and indirect permitted transitions, the electronic absorption spectra of pure PANI and complexed PANI show a substantial interaction. According to the results of the optical research, CdCl₂ doped PANI is a promising material for electrochromic and storage devices in solid state batteries.

Results show that CdCl₂ doped PANI samples are suitable candidates for solid state batteries, optoelectronic displays, electrochromic and storage devices.

REFERENCES

- [1] Bloom P. W. M., Vissenberg M. C. J. M., Hulberts J. N., Martens H. C. F., Schoo, H. F. *M. Appl Phys Lett* 2000, 77, 2057.
- [2] Kumar L, Dhawan S. K, Kamalsannan M. N, Chandra S, *Thin Solid Films* 2003, 441, 243.
- [3] Guatafson G. Cao Y, Treacy G. M, Klavetter F, Colaneri N, Heeger A. J, *Nature*, 1992,357, 477.
- [4] Verma A, Sexena K, Chanderkant S, Dhawan S K, Sharma R K, Sharma C. P, Kamalasannan M. N, Chandra S., *J Biochem Biotechnol* 2001, 96, 215.
- [5] Genies E. M, Hany P, Santier C, *J Appl Electrochem* 1988, 18, 751.
- [6] Kulkarni V. G, Mathew W. R, Campbell J. C, Dinkins C. J, Durbin P. J, In *The 49th ANTEC Conference Proceedings, SPEP Engi, Montreal, Canada, May 5–9, 1991*; p 663.
- [7] Yogeesh N, "Graphical representation of Solutions to Initial and boundary value problems Of Second Order Linear Differential Equation Using FOOS (Free & Open Source Software)-Maxima", *International Research Journal of Management Science and Technology (IRJMST)*, 5(7), 2014, 168-176
- [8] Osaheni J. A, Jenekhe S. A, Vanherzeele H, Meth J. S, Sun Y, MacDiarmid A. G, *J PhysChem* 1992, 96, 2830.
- [9] Kobayashi T, Yoneyama H, Tamura H, *J Electroanal Chem* 1984, 161, 419.
- [10] Paul E. W, Ricco A. J, Wrighton M. S, *J PhysChem* 1985, 89, 1441.
- [11] F. Garten, J. Vrijmoeth, A.R. Schlatmann, R.E. Gill, T.M. Klapwijk, G. Hadziioan-nou, *Synth. Met.* 76 (1996) 85.
- [12] H.L. Wang, F. Huang, A.G. Mac Diarmid, Y.Z. Wang, D.D. Gebler, A.J. Epstein, *Synth. Met.* 80 (1996) 97.
- [13] H. Sangodkar, S. Sukeerthi, R.S. Srinivasa, A. Lal, *Anal. Chem.* 68 (1996) 779.
- [14] C. Arbizzani, M. Mastragostino, B. Scrosati, *Hand Book of Organic Conductive Molecules and Polymers*, John Wiley&Sons Inc., New York, 1997 (Chapter 11), p. 595.
- [15] C.J. Mathai, S. Saravanan, M.R. Anantharaman, S. Venkatachalam, S. Jayalek-shmi, *J. Phys. D: Appl. Phys.* 35 (2002) 240.
- [16] Huang W. S, Humphrey B. D, MacDiarmid A. G, *J. Chem.Soc., Faraday Trans.* 1986, 82, 2385.
- [17] J B M Krishna^{1,4}, A Saha¹, G S Okram², S Purakayastha³ and B Ghosh³ *J. Phys. D: Appl. Phys.* 42 (2009) 115102
- [18] Sadia Ameen^{1,2}, G B V S Lakshmi¹ and M Husain *J. Phys. D: Appl. Phys.* 42 (2009) 105104.
- [19] Jiaying Huang,[†] James A. Moore,[‡] J. Henry Acquaye,[‡] and Richard B. Kaner, *Macromolecules* 2005, 38, 317-321.
- [20] A.J. Epstein, J.M. Ginder, F. Zuo, R.W. Bigelow, H.S. Woo, D.B. Tanner, A.F. Richter, W.S. Huang, A.G. MacDiarmid, *Synth. Met.* 18 (1987) 303.

- [21] M.G. Roa, J.M. Ginder, T.L. Gustafson, M. Angelopoulos, A.G. MacDiarmid, A.J. Epstein, Phys. Rev. B 40 (1989) 4187.
- [22] R.P. McCall, J.M. Ginder, J.M. Leng, H.J. Ye, S.K. Manohar, G.E. Austers, G.E. Asturias, A.G. MacDiarmid, E.J. Epstein, Phys. Rev. B 41 (1990) 5202.
- [23] Reddy, M.J., Chu, P.P., and Rao, U.V.S. (2006) J. Power Sourc., 158 (1): 624.
- [24] Anantha, P.S. and Hariharan, K. (2005) J. Solid State Ionics., 176: 155.–13.
- [25] Hodge, G.H., Edward, G.P., and Simon, J. (1996) Polymer, 37: 1371.
- [26] Reddy, M.J., Chu, P.P., and Rao, U.V.S. (2006) J. Power Sourc., 158 (1): 624.
- [27] Madhu Mohan V, Raja V, Sharma AK, Narasimha Rao VVRN (2004) Mater Chem Phys 94:177.
- [28] KKMaurya, N.Srivastava, S.AHashmi, S.Chandras, J Mat.Sci., 27(1992),.6357.
- [29] Jianbo Yin, Xiang Xia, Liqin Xiang, Yinpo Qiao and Xiaopeng Zhao Smart Mater. Struct. 18 (2009) 095007 (11pp).
- [30] Donghui Zhoua; Srinivas Subramaniamb; James E. Mark, Journal of Macromolecular SciencePart A-Pure and Applied Chemistry, 42:113–126, 2005.
- [31] G.M. Thutupalli and S.G. Tomlin, J. Phys. D Appl. Phys. 9 (1976) 1639.
- [32] V. Raja, V. M. Mohan, A. K. Sharma, V. V. R. Narasimha Rao, Ionics DOI 10.1007/s11581- 008- 0281-5.
- [33] Mott, N.F.; E.A.Davis.; Electronic process in Non-crystalline Materials. 2nd Edn. Clarendon Press Oxford, U.K. 1979.
- [34] N.F. Mott and E.A. Davis, Electronic Processes in Non-Crystalline Materials, Oxford, Clarendon, 1979.
- [35] F. I. Ezema, A. B. C. Ekwealor, P. U. Asogwa, P. E. Ugwuoke, C. Chigbo and R. U. Osuji, Turk J Phys 31 (2007) , 205 – 210.
- [36] A.M. Abdul-Kader, Philosophical Magazine Letters Vol. 89, No. 3, March 2009, 162–169.
- [37] Yogeesh N, "Solving Linear System of Equations with Various Examples by using Gauss method", International Journal of Research and Analytical Reviews (IJRAR), 2(4), 2015, 338-350